201974: gold grain, Carlow Castle prospect

(Roebourne Group, Karratha Terrane)

Sample type	Gold grain
Total weight	0.5 g
Sample location	Carlow Castle prospect, about 26 km east-southeast of Karratha
Coordinates	MGA zone 50, 507850E 7698457N
Datum	GDA94
1:250 000 map sheet	ROEBOURNE (SF 50-3)
1:100 000 map sheet	ROEBOURNE (2356)
Tenement	E 47/1797
Collector	Artemis Resources

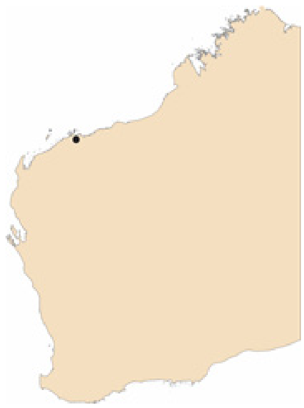

Location and sampling

The sample was provided by Artemis Resources in January 2019. It was collected from a sulfide breccia fill in a mafic rock at the Carlow Castle prospect, in the northwest Pilbara region (Artemis Resources, 2019, written comm., 11 January).

Geological context

The Carlow Castle prospect is located about 1.3 km south of the southern segment of the Regal Thrust, in the Roebourne greenstone belt of the Karratha Terrane and the intrusive 3024–3007 Ma Orpheus Supersuite, northwest Pilbara Craton. The thrust is a regionally significant fault spatially associated with numerous shear-hosted gold and copper deposits in the Roebourne Group and the Nickol River Formation (e.g. Lower Nickol, Weerianna, Carlow Castle, Sing Well; Hickman, 2002, 2016; GSWA, 2020). The local bedrock includes metamorphosed massive and pillowed basalt, locally fine-grained spinifex-textured komatiitic basalt of the 3280–3270 Ma Weerianna Basalt, Roebourne Group. The serpentinized peridotite and dunite of the 3023–3007 Ma Andover Intrusion, Orpheus Supersuite are located immediately to the south-southeast of the sample locality (Hickman, 2022a,c; GSWA, 2020).

The Carlow Castle prospect is about 1 km east-southeast of the Carlow Castle gold–copper–cobalt deposit, where mineralization occurs in a primary sulfide zone and an overlying supergene-enriched zone. At the Carlow Castle deposit the primary sulfide mineralization is structurally controlled, occurring in sulfide-rich quartz–carbonate veins within a tectonized zone. On the southern side of the Regal Thrust, within a tectonized zone, there is also extensive chlorite-silica alteration throughout the mafic to ultramafic volcano-sedimentary sequence of the 3280–3261 Ma Ruth Well Formation, Roebourne Group (Fox et al., 2019; Hickman, 2022b, 2016). The Greater Carlow Project has an inferred mineral resource as at 13 October 2022 of 8.74 Mt at 2.5 g/t Au, 0.73% Cu and 0.09% Co (Artemis Resources, 2022).

The nearest regolith landforms are an alluvial–fluvial unit comprising unconsolidated gravel, sand, silt, and clay in active but poorly defined drainage channels on floodplains, and a colluvial unit comprising unconsolidated sand, silt, and gravel in outwash fans, scree and talus, and proximal mass-wasting deposits (GSWA, 2020).

Methodology

The gold sample was photographed and weighed, and its overall morphology and external features, such as colour, roundness, surface relief, coatings, mineral inclusions and mineralogical assemblages, were recorded using visual morphometry. The raw surface of the sample was analysed using scanning electron microscopy with energy dispersive X-ray system (SEM-EDS). The sample was then mounted in epoxy resin, cut and polished and the gold grain microstructure and inclusions were examined using optical and SEM-EDS analyses. Gold microchemistry was determined by laser ablation inductively coupled plasma mass spectrometry (LA-ICP-MS), calibrated against certified gold reference materials (CRM; Murray, 2009). The sample was ablated in triplicate along 0.5 mm-long traverses and average values calculated for elements present in the CRM. The gold surface was repolished after laser ablation, etched with aqua regia, and its internal structure examined using reflected-light microscopy and SEM-EDS. Then the surface was repolished again using ion beam milling, and the gold grain microstructure verified using electron back-scattered diffraction (EBSD) analysis. Details of this method are described in Hancock and Beardsmore (2020).

Morphology

The gold grain is moderately rounded and flattened but lumpy, with dimensions 8 × 4 × 2 mm. It is covered by ferruginous clays (Fig. 1).

Figure 1. Sample 201974: gold grain, Carlow Castle prospect

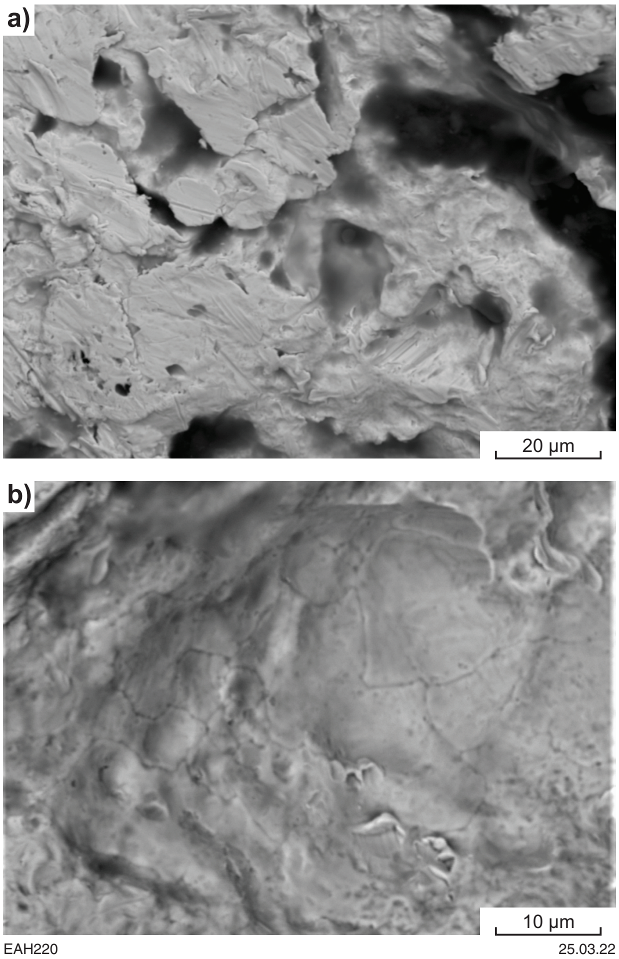

Figure 2. Backscattered electron images of sample 201974: gold grain, Carlow Castle prospect

SEM-EDS analysis of raw surfaces

The surface of the grain is scratched and compacted, and contains no detectable Ag (Fig. 2a). A fine-grained (3–12 µm), honeycomb-like polygranular microstructure is visible in the gold in some cavities in the nugget surface (Fig. 2b).

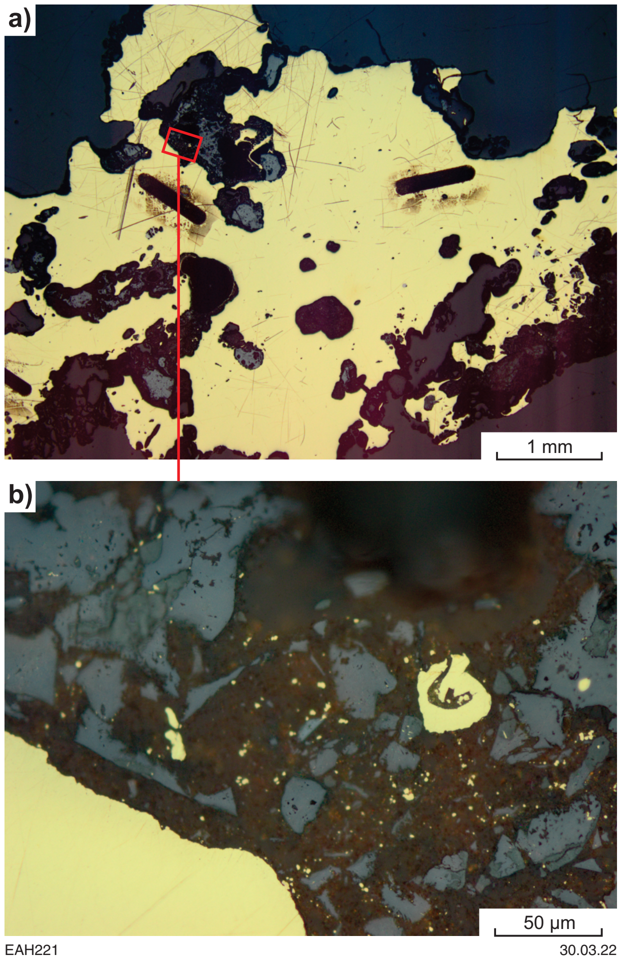

Figure 3. Reflected-light photomicrographs of polished surface of sample 201974: gold grain, Carlow Castle prospect. Dark, elongate lines are laser ablation tracks produced during LA-ICP-MS analyses

Optical microscopy of polished surfaces

In section, the irregular surface of the gold grain is evident, as there are many interior voids and cavities that are filled by Fe-oxide minerals and clays containing finely disseminated, rounded gold nanoparticles (Fig. 3a,b).

SEM-EDS analysis of polished surfaces

The main gold mass contains 6.5% Ag, and several pyrrhotite inclusions. One relatively large (up to 70 µm), euhedral pyrrhotite crystal contains 0.5% Ni (Fig. 4a). Several smaller, irregular pyrrhotite grains are associated with illite flakes and calcite grains (Fig. 4b). Discoidal nanoparticles of pure gold and larger, rounded quartz grains are dispersed through goethite–illite–Fe chlorite–calcite–kaolinite clay mixtures filling cavities in the gold (Fig. 4c).

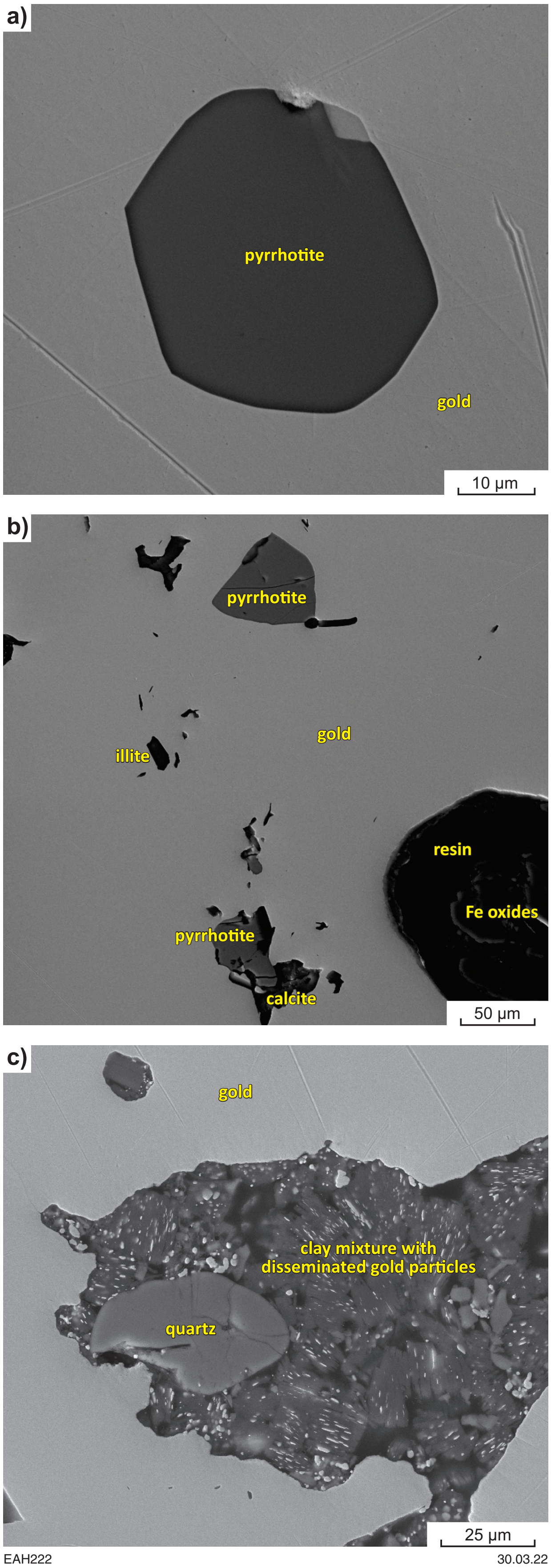

Figure 4. Secondary electron images of mineral inclusions in sample 201974: gold grain, Carlow Castle prospect

LA-ICP-MS analysis

Analyses consistently detected Ag, Cu and Hg within the gold, in concentrations higher than the instrumental detection limit, and probably occurring as limited solid solutions in the gold. Other trace elements were detected only sporadically in low (sub-ppm) concentrations, possibly occurring in micro- and nano-inclusions.

The gold grain contains moderate amounts of Ag (6%), Cu (326–361 ppm) and Hg (236–243 ppm) (Table 1). Elevated Ni, Zn and Sb (sub-ppm) are associated with very high Na concentrations in two of the three analytical traverses (Table 2), and most likely came from regolith clays that were inadvertently ablated. Magnesium was detected in all three traverses, and elevated concentrations of Bi and Sn (in ppb) were measured in the traverse without Na.

Table 1. LA-ICP-MS data for selected elements in sample 201974: gold grain, Carlow Castle prospect

Ag (%)	*Cu (ppm)*	*Hg (ppm)*	*Other (ppm)*
5.8, 5.9, 6.3	326, 342, 361	236, 242, 243	Na, Mg, Ni, Zn, Sb, Bi, Sn

Acid etching

The primary microstructure of the gold grain is coarsely polycrystalline with simple twinning (Fig. 5a). Some crystal boundaries are curved and show partial granulation and incipient disintegration, particularly in the outermost 5–10 µm thick rim of the grain (Fig. 5b). There are many very small intergranular veinlets and marginal rims of pure Au (Fig. 5b,c).

SEM-EBSD analysis

To verify the acid etching results, the surface of the gold grain was polished again, etched using ion-beam milling and analysed using SEM-EBSD. This revealed a strongly deformed, recrystallized microstructure comprising a poly-granular fabric with uneven crystal size – larger in the centre and smaller in the outer parts and around voids and inclusions (Fig. 6a,b). Many crystal are damaged and have diffused, rounded, smooth or irregular boundaries. The outer rim with grain size < 100 µm is partly granulated (Fig. 6a,b), and the outermost 5–10 µm thick rim shows granulation and disintegration (Fig. 6c). A line crossing the main crystal on the Figure 6c is the laser ablation track produced during LA-ICP-MS analysis.

Interpretation

The primary gold grain has a coarse polycrystalline structure, and contains 6% Ag and pyrrhotite inclusions, suggesting a hydrothermal origin. The recrystallization and partial granulation probably indicate some post-depositional deformations and metamorphic impacts to the primary microstructure. The grain was subsequently eroded, mechanically abraded along outer rim during transportation, then buried in a regolith environment where it experienced some dissolution and accumulation of Fe oxides–illite–chlorite–calcite–kaolinite and pure gold nanoparticles in resulting cavities.

Table 2. LA-ICP-MS compositional data for sample 201974: gold grain, Carlow Castle prospect

Laser ablation track	*Unit*	^{7}Li	^{9}Be	^{11}B	^{23}Na	^{25}Mg	^{27}Al	^{29}Si	^{44}Ca	^{45}Sc	^{49}Ti	^{51}V	^{53}Cr	^{55}Mn	^{57}Fe	^{59}Co	^{60}Ni	^{65}Cu
1	cps		2	10	35581	258	537		82		7			167		7	145	42314
2	cps					121	273		28		7	3	2	9	20	6	16	40400
3	cps			134	289016	326	507		276		5	3		51		5	195	44630
1	ppm					3.09					0.15						1.46	342
2	ppm					1.44					0.14						0.16	326
3	ppm					3.91					0.11						1.97	361

Laser ablation track	*Unit*	^{66}Zn	^{69}Ga	^{72}Ge	^{75}As	^{82}Se	^{85}Rb	^{88}Sr	^{89}Y	^{90}Zr	^{93}Nb	^{98}Mo	^{101}Ru	^{103}Rh	^{108}Pd	^{109}Ag	^{111}Cd	^{115}In
1	cps	70	2	5	3	1	15	17	2	6	780			2	6	12180838	41	3
2	cps	29	4		4		7	17	2		14	2			4	12951886	38	7
3	cps	102					32	28		7	331	1	1	2	5	11851267	43	2
1	ppm	0.80			0.04	0.08								0.004	0.04	59102		0.006
2	ppm	0.33			0.04										0.03	62843		0.013
3	ppm	1.17												0.005	0.03	57503		0.004

Laser ablation track	*Unit*	^{120}Sn	^{121}Sb	^{126}Te	^{133}Cs	^{138}Ba	^{139}La	^{140}Ce	^{141}Pr	^{145}Nd	^{151}Eu	^{157}Gd	^{159}Tb	^{162}Dy	^{165}Ho	^{167}Er	^{169}Tm	^{172}Yb
1	cps	107	558		2	7	2						1					
2	cps	172	76	2	2	6				1							1	
3	cps	111	832		1	7		2				1		1				
1	ppm	0.48	2.17															
2	ppm	0.77	0.29	0.04														
3	ppm	0.50	3.24															

Laser ablation track	*Unit*	^{175}Lu	^{178}Hf	^{181}Ta	^{182}W	^{185}Re	^{189}Os	^{193}Ir	^{195}Pt	^{202}Hg	^{205}Tl	^{208}Pb	^{209}Bi	^{232}Th	^{238}U
1	cps			64						70364	1	11	60		44
2	cps			4	1					68534	3	15	253		3
3	cps			24		1				70180	1	14	47	1	15
1	ppm									243		0.03	0.128		
2	ppm									236		0.05	0.538		
3	ppm									242		0.04	0.100		

Notes: cps, count per second; ppm, parts per million

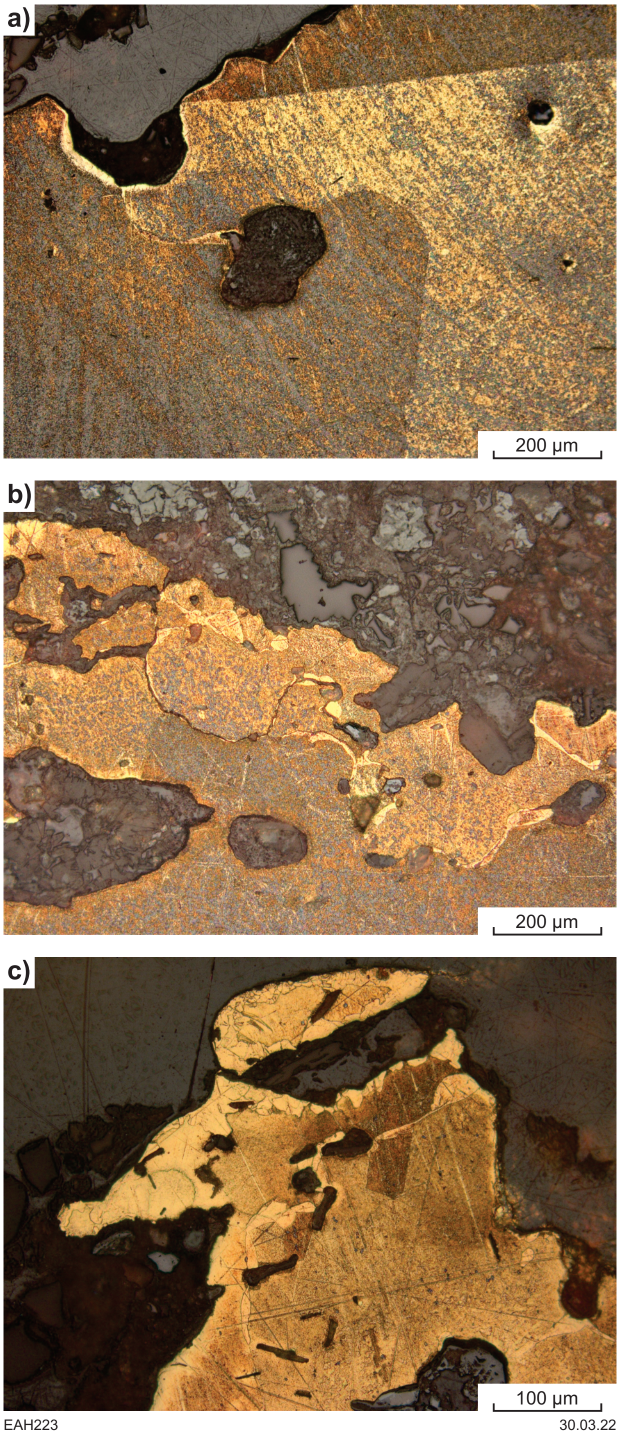

Figure 5. **Reflected-light photomicrographs, after repolishing and acid etching, of parts of sample 201974: gold grain, Carlow Castle prospect**

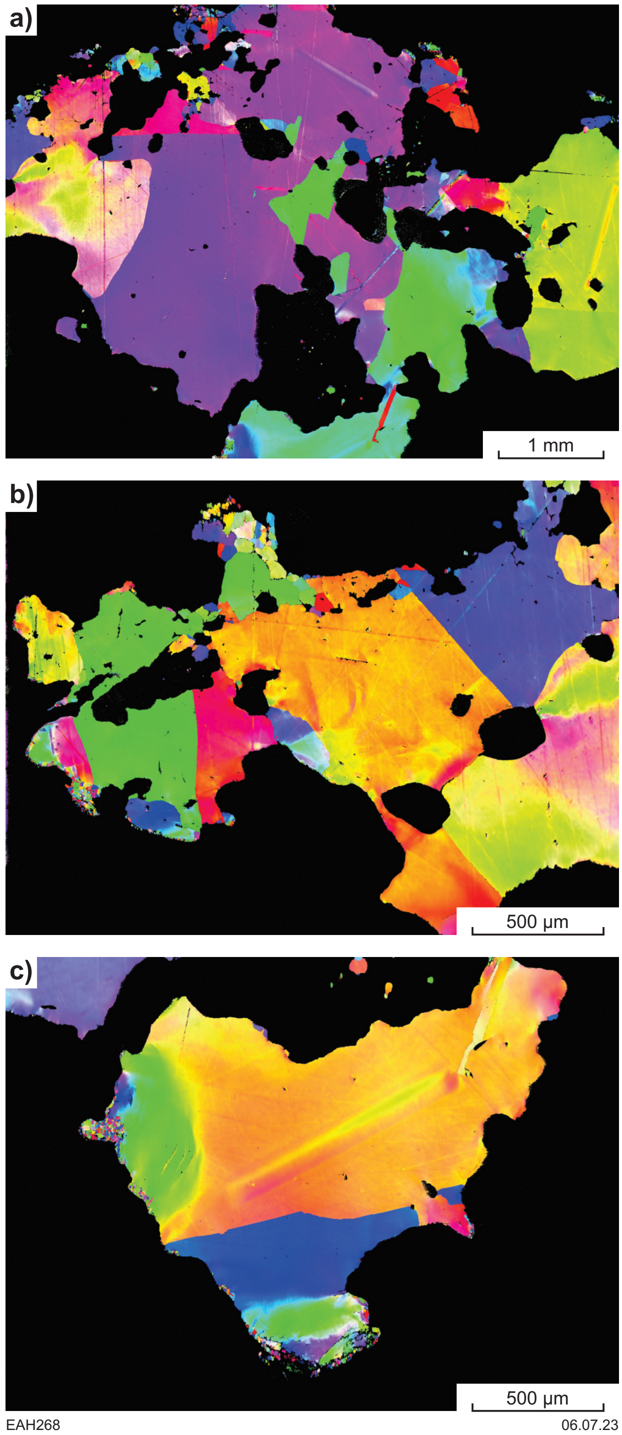

Figure 6. **Electron back-scattered diffraction (EBSD) images of repolishing surface of parts of sample 201974: gold grain, Carlow Castle prospect**

References

Artemis Resources 2022, High-Grade Gold Copper Cobalt Inferred Mineral Resource Lays Foundation for a Robust Greater Carlow Project (media release): Australian Securities Exchange (ASX), released 13 October 2022, 41p.

Fox, DCM, Spinks, SC, Pearce, MA, Barham, M, Le Vaillant, M, Thorne, RL, Aspandiar, M and Verrall, M 2019, Plundering Carlow Castle: first look at a unique Mesoarchean-hosted Cu–Co–Au deposit: Economic Geology and the Bulletin of the Society of Economic Geologists, v. 114, no. 6, p. 1021–1031, doi.org/10.5382/econgeo.4672.

Geological Survey of Western Australia 2020, Northwest Pilbara, 2020: Geological Survey of Western Australia, Geological Information Series, data package.

Hancock, EA and Beardsmore, TJ 2020, Provenance fingerprinting of gold from the Kurnalpi Goldfield: Geological Survey of Western Australia Report 212, 21p.

Hickman, AH 2002, Geology of the Roebourne 1:100 000 sheet: Geological Survey of Western Australia, 1:100 000 Geological Series Explanatory Notes, 35p.

Hickman, AH 2016, Northwest Pilbara Craton: A record of 450 million years in the growth of Archean continental crust: Geological Survey of Western Australia, Report 160, 104p.

Hickman, AH 2022a, Andover Intrusion (A-OPan-xo-a): Geological Survey of Western Australia, WA Geology Online, Explanatory Notes extract, viewed 11 April 2022, <www.dmirs.wa.gov.au/ens>.

Hickman, AH 2022b, Ruth Well Formation (A-ROr-xb-u): Geological Survey of Western Australia, WA Geology Online, Explanatory Notes extract, viewed 8 April 2022, <www.dmirs.wa.gov.au/ens>.

Hickman, AH 2022c, Weerianna Basalt (A-ROw-b): Geological Survey of Western Australia, WA Geology Online, Explanatory Notes extract, viewed 11 April 2022, <www.dmirs.wa.gov.au/ens>.

Murray, S 2009, LBMA certified reference materials. Gold project final update: The London Bullion Market Association, Alchemist, no. 55, p. 11–12.

Recommended reference for this publication

Hancock, EA, Blay, OA and Beardsmore, TJ 2023, 201974: gold grain, Carlow Castle prospect; GSWA Mineralogy Record 8: Geological Survey of Western Australia, 6p.